International Journal of Design & Nature and Ecodynamics
Vol. 21, No. 2, February, 2026, pp. 425-436
Journal homepage: http://iieta.org/journals/ijdne

Bio-Composite Formulations Based on Natural Binders for Treating Hollow Palm Trunks: Mechanical, Thermal, and Microstructural Evaluation

Shireen Hasan Challoob[1], Aous Abdulhussain Moyet[2], Ahmed Subhi Abbas[3], Ahmed Hafedh Mohammed[1], Kadhim K. Resan[1], Ali M. Flayyih[1], Mohammed Ali Abdulrehman[1,4*]

[1] Department of Materials Engineering, College of Engineering, Mustansiriyah University, Baghdad 10045, Iraq
[2] Department of Civil Engineering, University of Baghdad, Baghdad 10070, Iraq
[3] Department of Civil Engineering, College of Engineering, Al-Mustafa University, Baghdad 10045, Iraq
[4] School of Materials and Mineral Resources Engineering, Universiti Sains Malaysia, Nibong Tebal 14300, Malaysia

Corresponding Author Email: mohammed_ali_mat@uomustansiriyah.edu.iq

https://doi.org/10.18280/ijdne.210211

Received: 13 December 2025
Revised: 11 February 2026
Accepted: 26 February 2026
Available online: 28 February 2026

Keywords:
bio-composites, gum arabic, natural rubber latex, wood sawdust, rice husk, sustainable

ABSTRACT

The objective of this study was to develop an eco-friendly biocomposite material suitable for thermal insulation and rehabilitation applications by utilizing agricultural waste materials and bio-based adhesives. In this study, three different types of bio-based adhesives, plant-based glue (PG), gum arabic (GA), and natural rubber latex (LX), were used to prepare composites with wood sawdust (WS) and rice husk (RH) materials. Twelve different formulations were produced with different filler/binder ratios (70/30 and 60/40). The experimental results showed that the GA/WS composite with a filler/binder ratio of 60/40 had a dense and compact microstructure, achieving a compressive strength value of 5.8 MPa, with reduced water absorption at 8.1%. In contrast, the LX/RH composite with the same filler/binder ratio showed a porous and elastic microstructure, achieving a reduced thermal conductivity value of 0.115 W/m·K, with improved adhesion properties (2.15 MPa) and minimal shrinkage (0.70%). Microstructure analysis by Scanning Electron Microscopy (SEM) showed good interfacial adhesion in the GA/WS composites, while a flexible polymer network was observed in the LX/RH composites. Moreover, FTIR analysis showed that the filler/binder interactions were mainly governed by physical bonding mechanisms, without any new chemical compound formation. Therefore, the experimental results showed that the properties of the biocomposites could be improved by choosing the most suitable filler/binder combinations. GA/WS composites are recommended for applications where better mechanical properties and reduced permeability are required, while LX/RH composites are recommended for use in thermal insulation and rehabilitation applications.

1. INTRODUCTION

The construction industry is increasingly prioritizing sustainability and the reduction of environmental impacts worldwide. This trend has accelerated the search for alternative materials that can deliver reliable structural performance while reducing depletion of natural resources and greenhouse gas emissions. Traditional construction materials, such as steel and concrete, although necessary in contemporary buildings, are major contributors to the environmental impact. Therefore, more attention has been paid to alternative material systems, which are relevant to the principles of circular economy and low-carbon development [1]. Bio-composite materials based on renewable resources (especially agricultural wastes such as rice husks (RH) and wood sawdust (WS)) have become potential alternatives. In addition to providing adequate mechanical and thermal performance, these materials contribute to waste utilization and environmental protection [2, 3]. WS and RH are readily available, and under normal circumstances, they are disposed of through open burning or dumping. The disposal of WS and RH through open burning or dumping results in environmental pollution and waste of valuable resources. The use of WS and RH as biocomposite fillers is a viable waste management strategy, which also provides a means of producing composite materials with good properties [4]. These fillers can be used in combination with bio-based binders, including starch, bio-based resins, and natural latex (LX). The choice of these materials is based on their availability, compatibility, and physical and chemical properties, especially the fibrous structure of WS and silica in RH, as well as the bonding properties of the chosen natural binders. These bio-based binders exhibit good mechanical and physical properties [5, 6]. Composites exhibit good biodegradability, lightness, and recyclability, as required by the principles of green engineering [7]. However, their durability, properties, and practical applications in structural rehabilitation have not been adequately explored [8].

The application of bio-based composites for fixing damaged and hollow date palm trunks in arid environments is one of the few applications cited in the literature. Date palm trunks, which have structural and geometric properties that allow them to be used in lightweight construction, are discarded when degraded [9, 10]. The trunks are hollow and porous, which means that to restore their properties, fillers must be used. The fillers can be created using a bio-based composite, which is environmentally friendly and composed of locally sourced materials such as sawdust and RH. However, limited literature has been devoted to addressing this application, especially when the environment is arid, which means there is a gap in the literature, which this study will address [7, 8, 11]. It has already been proven that the use of wood/RH fillers in composites may enhance the dimensional stability, decrease the absorption of water, and increase the compressive, flexural, and tensile properties of the composites [2, 5, 12]. The type and percentage of binder have a substantial impact on the behavior of the composites. They affect the interfacial bond between the binder and fillers and the transfer of loads between the particles. These formulations may enhance cohesion, decrease cracking, and increase environmental compatibility [3, 6, 13]. Other critical parameters that affect the performance of these composites include density, thermal insulation capacity, moisture content, and biological degradation resistance [9, 14]. The application of biocomposites is strongly linked to the idea of the circular economy, which allows for a reduction in resource consumption and improvement in material utilization [9, 15]. The application of agricultural residues allows for a reduction in external resources, production costs, and regional sustainability [16]. Moreover, they could be effective tools for carbon emission reduction by replacing traditional cement or synthetic systems. However, their durability under varying environmental conditions, such as temperature, humidity, and ultraviolet light, is not well understood and needs to be verified under practical conditions [10, 17]. There are further advantages to the concept of co-fillers, which use sawdust and RH. The complementary properties of these materials, that is, the presence of cellulose fibers in sawdust and silica content, will improve the bonding between them [2, 5, 18]. However, variations in the properties of materials, as well as curing, will affect their efficiency, hence the need for optimal processing of materials [3, 4, 19]. Another approach that has been proposed as a means of combining traditional materials and sustainable technology is the use of reinforcing bio-composite fillers in hollow trunks of date palm trees. This will help reduce the use of cementitious or man-made repair materials by using agricultural waste in the form of structural solutions [8, 10]. This can help attain environmental sustainability and economic development, reduce construction costs, and stimulate innovation [11]. To this end, this study aims at the preparation and overall assessment of environmentally sound biocomposite fillers made from WS and RH using natural binding agents, such as plant-based glue (PG), gum Arabic (GA), and LX. The main aims were to determine the best mix compositions, evaluate their mechanical, physical, and durability-related characteristics, and compare their performances with those of traditional synthetic repair materials. Special focus is given to assessing their performance in strengthening and rehabilitating hollow date palm trunks, thus offering a locally available and sustainable alternative to non-biodegradable materials [1-5]. This selection allows for the systematic evaluation of binder-filler interactions as well as their impact on the overall performance of the developed composites. This research focuses on environmental sustainability, structural engineering, and materials science. This study will contribute to the development of sustainable construction materials by presenting the possibility of using renewable and biodegradable materials for structural applications [6-10]. Additionally, the research will contribute to the development of the circular bio-economy through the utilization of locally sourced agricultural wastes, thereby reducing the environmental impacts, energy consumption, and carbon emissions. This study is expected to contribute to the development of lignocellulosic composite technologies that can be utilized for rehabilitation and construction work in a sustainable way [11-16]. Notably, the proposed study provides an engineering application through the combination of bio-composite materials and in situ structural rehabilitation of hollow natural palm trunks, for which limited research attention has been reported in the literature. However, the research did not compare the impact of different natural binder materials and fillers on the microstructure–property relationship, particularly for structural rehabilitation under arid environmental conditions. In contrast to other research in this area, in which the authors mainly focused on the development of materials, the proposed study focuses on a practical problem for structural applications under real service conditions. The proposed study will contribute to filling the gap between the development of materials and their application to structures, especially in the Middle East and Iraq, where palm trees are abundant. This study provides a combination of binder type, filler morphology, interaction effects, and their relationship to the overall performance of the materials. This technology will provide practical applications for the development of biocomposites for sustainable construction and landscaping projects [20]. In conclusion, the production of these biocomposite fillers provides an answer to the call for sustainable materials that can function as structural performance elements while simultaneously being compatible with the environment. The findings showed that functional performance and environmental considerations can be achieved by designing engineering solutions based on natural resources. This paper demonstrates the possibility of developing sustainable structural repair materials and thus supports the idea that environmental responsibility and structural performance can be integrated in engineering.

2. METHODOLOGY

Two different natural fillers were utilized for the development of biocomposites. WS was collected from the carpenter workshops near the university campus. Then, it was sieved to a particle size of less than 1 mm. Then, it was dried at 105 ℃ for 24h using an oven to eliminate the moisture content. RH was dried at 105 ℃ for 24 h using an oven after grinding to a fine powder with an average particle size of less than 1mm. Many lignocellulosic compounds, such as Cellulose, Hemicellulose, and Lignin, are present in natural fillers. RHs are less likely to be attacked by bacteria because of the high amount of silica present. Therefore, they can easily absorb water. Three natural binders were used to bond the natural fillers. One of the natural binders utilized in the present study is GA. It is derived from the bark of Acacia Senegal trees. It was dissolved in water at 15 wt.% at room temperature

(~25 °C) under continuous stirring for 30 min until complete dissolution occurred. It acts as a thick bioresin. PG is derived from a solution containing 10% starch. Corn starch was used as the starch source. The solution was heated at 90 °C under continuous stirring. LX is a commercial natural rubber latex (NRL). This is a water-based binder. It is used to bond natural fillers. It is utilized to bond natural fillers because it has the characteristics of film-formers. It was filtered using a fine mesh filter under continuous stirring to prevent coagulation. Then 1 wt.% of ammonia was added to it for stabilization. All natural binders were reusable, biodegradable, and compatible with lignocellulosic materials. Hence, they were utilized for the development of biocomposites.

The effects of the natural binders and their fractions of natural binders at two different levels for each natural filler were investigated (Table 1). For each natural binder, two different ratios of natural filler to natural binder were calculated. The two different ratios of the natural binders were FB-L: 70:30 (weight percent) and FB-H: 60:40 (weight percent). Hence, 12 different mixes of natural biocomposites were prepared. Water was gradually added to the mixture to obtain a workable consistency. To obtain a workable consistency for all the mixes, the water-binder mass ratio was varied between 0.25 and 0.35.

Table 1. Mix the matrix with two binder fractions per binder for each filler (full-factorial design)

Group	Mix Code	Filler	Binder	Filler: Binder (wt.%)	Level
A (WS)	A1	WS	PG	70:30	FB-L
A (WS)	A2	WS	PG	60:40	FB-H
A (WS)	A3	WS	GA	70:30	FB-L
A (WS)	A4	WS	GA	60:40	FB-H
A (WS)	A5	WS	LX	70:30	FB-L
A (WS)	A6	WS	LX	60:40	FB-H
B (RH)	B1	RH	PG	70:30	FB-L
B (RH)	B2	RH	PG	60:40	FB-H
B (RH)	B3	RH	GA	70:30	FB-L
B (RH)	B4	RH	GA	60:40	FB-H
B (RH)	B5	RH	LX	70:30	FB-L
B (RH)	B6	RH	LX	60:40	FB-H

Notes: WS: wood sawdust; RH: rice husk; PG: plant-based glue; GA: gum arabic; LX: natural latex; FB-L: low binder fraction (70:30); FB-H: high binder fraction (60:40).

Table 2. List of experimental tests and their ASTM standards

Property	Test Method	Standard Reference
Bulk density	Determination by mass/volume ratio	ASTM C642
Water absorption	Immersion test (24 h)	ASTM C642
Compressive strength	Load at failure/cross-section	ASTM D695
Adhesion to wood	Pull-off test	ASTM D4541
Linear shrinkage	Dimensional change after drying	ASTM C531
Thermal conductivity	Guarded hot plate method	ASTM C177

The fillers and binder were manually mixed for ten minutes until all materials were the same. The mixture was then placed in a cylindrical mold (50 mm × 50 mm) and compacted lightly to remove air bubbles. The curing process had two stages: air drying at room temperature (25 ± 2 °C) for 24 h and ventilated curing at 35 °C for seven days to facilitate polymerization of the binder and stabilization of the moisture. The mixture was removed from the mold and left at room temperature before the tests were conducted.

Table 2 summarizes all the physical and mechanical tests performed according to the respective ASTM standard. The average values were obtained from three tests performed for each parameter to ensure that the tests were repeatable, and the results were reported as mean values.

Thermal property and microstructure analyses were performed using advanced material characterization techniques. The pore distribution and interface between the fillers and binder were studied using Scanning Electron Microscopy (SEM). The functional groups were identified using Fourier Transform Infrared Spectroscopy. Using this tool, the absence of chemical reactions between the fillers and binder was also confirmed, indicating the presence of only physical interactions such as hydrogen bonding. The composite material was subjected to various temperature conditions using differential scanning calorimetry (DSC) and thermogravimetric analysis (TGA). TGA was mainly used to check the stability of the materials in the temperature range of 55-60 °C, as the application does not require higher temperatures.

All mechanical and physical tests were carried out according to the respective ASTM standards, as specified in Table 2. The test samples were tested under controlled conditions. The results are the averages of three measurements for each test.

The adhesion strength was determined using a pull-off test, as specified by ASTM D4541. A loading fixture, that is, a dolly, was bonded perpendicular to the surface using an appropriate adhesive. The fixture was left to cure for 24 h. Before testing, the surface was cleaned to remove contaminants. Pull-off tests were performed using a portable adhesion tester. A tensile force was applied perpendicular to the surface at a constant rate that did not exceed 1 MPa/s until failure. The maximum force at which detachment occurred was noted. The adhesion strength was calculated by dividing the force by the area.

After laboratory evaluation of all 12 mixes, the two best mixes for each type of filler were chosen using a multicriteria index. Optimal WS and RH mixtures were injected into the hollow spaces of naturally rotted palm trunks using the tamping method. The sections were left for six months, during which time observations were performed to study the stability, adhesion, and cracking properties of the mix. Periodic observations were carried out to study the changes in moisture content and microcracks.

3. RESULTS AND DISCUSSION

This study addresses the mechanical, physical, thermal, and microstructural performance of eco-friendly biocomposite fillers and provides test results. The influence of the filler type (WS and RH), binder type (PG, GA, and LX and binder ratio (70:30 and 60:40) was investigated.

3.1 Discussion of compressive strength results

Table 3. Compressive strength results of the bio-composite fillers at 28 days

Mix Code	Compressive Strength (MPa)
A1	3.2 ± 0.12
A2	4.1 ± 0.15
A3	4.5 ± 0.18
A4	5.8 ± 0.20
A5	3.6 ± 0.14
A6	4.3 ± 0.16
B1	2.8 ± 0.10
B2	3.5 ± 0.13
B3	4.0 ± 0.15
B4	5.2 ± 0.19
B5	3.1 ± 0.11
B6	3.9 ± 0.14

Table 3 shows that the binder type and filler-to-binder ratio influenced the compressive strength of the biocomposite fillers. The obtained results were found to be 2.8 to 5.8 MPa, which falls within the normal range of lightweight lignocellulosic-based laminated composite as a rehabilitation and non-structural material [2, 6, 17]. The mechanical response indicates the compatibility of the shape of the filler used, the volume of space inside the material, and the compatibility of the binder with the filler. This observation was strongly confirmed through SEM analysis, where the GA-WS composites showed a dense and compact microstructure, along with fewer voids, thus enhancing the stress transfer and load-bearing capacity. It is known that all these factors affect bio-based composites [3, 12, 18]. The findings indicated that regardless of the series, mixtures that incorporated GA had the best compressive strength. For example, the compressive strength of gum arabic-wood sawdust (GA–WS) (A4) is 5.8 MPa, which is higher than that of LX–WS (A6), which recorded 4.3 MPa. GA, a complex polysaccharide hydrocolloid, forms a sticky network that enables the filler particles to stick to each other and evenly spread stress to promote a homogenous distribution of stress [19]. Owing to the large number of hydrogen-bonding sites created by its branched structure, the polymeric film was strong, despite having been cured. This behavior is also supported by FTIR analysis, where strong O-H interactions are indicative of enhanced hydrogen bonding, which improves the adhesion and mechanical properties. These results are also in line with the study conducted by Rahmani et al. [2], which proved the effectiveness of bio-adhesives on lignocellulosic composites with regard to the transfer of loads, indicating that gum-based bio-adhesives enhance load transfer in composites. Nonetheless, according to Pedreño-Rojas et al. [20], PG has a moderate compressive strength because of the brittle and partially crystalline starch film formed during drying [20]. Starch bonds well at a young age, although it exhibits elastic recovery to ensure that microcracks cannot spread when compressed. However, LX fractures more easily but with low strength values. In comparison to GA-based composite materials, LX-based composite materials indicated a reduction in compressive strength of 10-15%, thereby validating the low contribution of these composite materials in terms of compressive strength despite their enhanced flexibility. This may be attributed to the more porous and less rigid microstructure observed for the LX-based systems in the SEM images, which reduces the effective load transfer. Although it does not fully contribute to the load-bearing resistance, the latex binder generates a semi-elastic polymeric phase that is capable of absorbing energy by deformation. Similar trends were observed by Aman et al. [19], who found that blends of latex and starch were soft yet not strong during compression. In comparison to the two fillers, WS composites were always better than RH composites. For instance, the GA-WS material (5.8 MPa) exhibited 11.5% higher strength than that of the GA-RH material (5.2 MPa), thus emphasizing the positive influence of the fibrous form on stress transfer. The SEM images show that the fibrous and irregular nature of WS enhances its mechanical interlocking with the matrix, thus improving its compressive strength.The fibrous texture and irregular shape of sawdust particles contribute to the mechanical interlocking of the binder matrix and the existence of points of stress concentration, which increases the strength of WS-based samples [16, 17]. However, the smoother surface and increased silica content of the RH particles lowered the number of bonding sites and interfacial adhesion. This is further supported by the SEM observations, which indicate smoother particle surfaces and gaps between interfaces in the composites based on RH, resulting in weaker bonding. This is in agreement with the results of Hossein Rahmani et al. [2], who concluded that because pressed carbonized sawdust composites are more easily packed and less porous, they compress better than other agricultural wastes. Teuber [16] also confirmed that the shape of the particles and surface roughness are anisotropic and effective in determining the stress transfer and material homogenization in wood-plastic and bio-based composites. The 60:40 (FB-H) mixtures always performed better than the 70:30 (FB-L) mixtures. An increase in the binder content from 30% to 40% led to an improvement in the compressive strength by up to 20-25%, depending on the type of binder and filler used. This improvement is related to the microvoid reduction and matrix continuity improvement observed in the SEM image, which improves the stress distribution. An increased binder content led to a reduction in the number of voids and wetting of the filler surfaces. Consequently, the density of the matrix and the stress distribution were enhanced [12, 18]. The blends that had the best compressive strength were GA-WS (60:40) and GA-RH (60:40) with compressive strengths of 5.8 MPa and 5.2 MPa, respectively. This proves that an appropriate binder level does not increase the cohesion of the matrix when too much polymer is used, which could act as a weak phase. Following this, further addition of the binder is likely to reduce the stiffness because a continuous soft layer of the film would be formed, which has been demonstrated in polymer-fiber hybrid structures [13]. Thus, the mechanical performance depends mainly on the binder content, interfacial adhesion, and porosity instead of the inherent strength of the raw materials. The compressive strength in this study is comparable to or even greater than that of other available natural filler-binder combination objects, including wood-gypsum composites [20] and groundnut husk-epoxy composites [6]. These results suggest that the developed materials can potentially be extensively used in environmentally friendly infill and rehabilitation processes, particularly in cases where dimensional stability and a compressive load of moderate magnitude are required. This is because of their high sustainability and low density. This system has no synthetic polymers or cementitious binders, which, according to the goals of sustainable construction set by Fong et al. [13] and Aiduang et al. [3], is eco-friendly. The most favorable ones are

GA-WS (60:40) and GA-RH (60:40), which are easy to handle, utilize renewable resources, and exhibit desirable mechanical characteristics. Therefore, this is a good option for repairing and strengthening hollow date palm trunks in dry areas.

Overall, the SEM and FTIR results confirm that the enhanced compressive strength is controlled by the dense microstructure, quality of the interfacial bonding, and physical interactions between the binder and filler. This shows that GA-based composites are effective in enhancing the load-bearing capacity of hollow palm trunks, especially in structural rehabilitation applications.

3.2 Discussion of water absorption and density results

The bulk density and water absorption test results demonstrated that there was an obvious correlation between the nature of the binder and filler properties, as indicated in Table 4. The addition of more binder material to the 70:30 (FB-L) mixture than to the 60:40 (FB-H) mixture led to a denser material that was more compact with a lower open space in the matrix. For instance, increasing the binder composition from 30% to 40% led to a reduction in water absorption from 12.8% (A1) to 8.1% (A4), that is, a reduction of 36.7%, whereas the density increased from 1213 to 1306 kg/m³ (≈ 7.7% increase). This improvement was confirmed by the SEM images, where a higher binder content created a more compact matrix with fewer interconnected pores. These findings are also aligned with previous studies on natural biocomposites, which indicate that an increase in the binder fraction enhances particle encapsulation and reduces water penetration routes [2, 6, 12].

Table 4. Water absorption and density results of the biocomposite fillers at 28 days

Mix Code	Water Absorption (%)	Bulk Density (kg/m³)
A1	12.8 ± 0.4	1213 ± 15
A2	10.4 ± 0.3	1247 ± 18
A3	9.6 ± 0.3	1278 ± 20
A4	8.1 ± 0.2	1306 ± 22
A5	9.8 ± 0.3	1234 ± 17
A6	8.7 ± 0.2	1283 ± 19
B1	14.2 ± 0.5	1187 ± 14
B2	12.3 ± 0.4	1219 ± 16
B3	11.0 ± 0.3	1232 ± 17
B4	9.2 ± 0.2	1267 ± 19
B5	12.0 ± 0.4	1206 ± 15
B6	10.5 ± 0.3	1249 ± 18

LX mixtures have shown higher water absorption than GA-based mixtures. For instance, the water absorption of the GA/RH (B4) mixture was 9.2%, whereas the LX/RH (B6) mixture exhibited a higher value of 10.5%. This indicates that the resistance to moisture is relatively low in the latex-based composites. Although latex is inherently hydrophobic and forms a continuous polymeric film, the resulting microstructure may contain distributed pores that facilitate water penetration. Therefore, the overall water absorption behavior is governed more by the microstructural porosity than by the intrinsic hydrophobic nature of latex [19]. The SEM images further confirmed this phenomenon, where a dense and continuous latex film coated the filler particles, providing an effective barrier against water entry. This impermeable coating envelops lignocellulosic particles and considerably limits capillary action through the application of a stretchable barrier. Aman et al. [19] gave similar results whereby sealing and cross-linking the polymers, latex-based adhesives enhance the water resistance of surfaces.

The GA series absorbed less water than the PG, although it was slightly higher than that of the latex composites. For example, the water absorption of GA-based composite materials is 10–20% lower than that of PG-based composites under the same mixing conditions. This demonstrates the enhanced water resistance of GA-based composite materials. FTIR results also confirmed this phenomenon by showing strong peaks of the O-H functional groups that indicate hydrogen bonding interactions, which reduce connectivity but allow some degree of moisture uptake. Although the high effectiveness of cohesive bonding may lower the chances of connection between the pores and the diffusion of water in its polysaccharide backbone, the polysaccharide structure still allows the absorption of a certain amount of moisture in the presence of hydroxyl groups [12, 18]. On the other hand, the highest absorption values were recorded for the PG-based composites. This is because of the hydrophilic starch structure of these composites, which tends to absorb and retain moisture. Pedreño-Rojas et al. [20] also observed this phenomenon in wood waste-gypsum composites with starch-type binders.

The WS composites were much denser and less water-absorbing than the RH series. For example, the GA-WS (A4) material recorded a water absorption of 8.1%, which is approximately 22.9% lower than that recorded for the LX-RH (B6) material (10.5%), but with a higher density (1306 vs. 1249 kg/m³, ≈ 4.6% increase). This is directly related to the SEM observations, where WS has a fibrous and interlocked structure, which decreases the void connectivity and increases the matrix compactness. The reduced number of continuous pores was caused by the fibrous texture and irregular shape of the WS, which made it easy to tightly pack the particles and establish a solid mechanical bond with the binder. Nevertheless, the smoother the RH surface and the higher the silica content, the larger the microvoids and interfacial gaps, and thus the greater the ability of moisture to penetrate [5, 16]. In the SEM images of the RH-based composites, it is clear that the particle surfaces are smoother and interfacial gaps are visible, making the composites susceptible to moisture ingress. This is why RH-based composites possess slightly higher absorption values and slightly lower densities. As Rahmani et al. [2] explained, carbonized husk materials with greater quantities of silica and ash weaken the matrix bonds and leave room for more water infiltration.

The higher the binder content, the lower the absorption of the mixtures. This was due to the fact that the filler particles had a coating that was thicker and more uniform, and therefore limited diffusion of water and blocked capillary pores. On the other hand, an increase in the amount of binder resulted in an average reduction of water absorption by 25-35%, while an increase of 5-8% was also recorded in density. This trend is in agreement with the SEM results, which showed reduced porosity and enhanced particle encapsulation with increased binder content. This also enhanced the bulk density, which signified the enhanced consolidation of the composite matrix. The reduced binder content in the FB-L (70:30) mixtures indicated that the porosity of the mixtures was more interconnected and allowed moisture to pass through them more easily. This is consistent with the studies conducted by Jeeva et al. [6] and Fong et al. [13], which stated the importance of the void ratio and continuity of the polymeric matrix in creating hybrid natural composites for the

determination of their density and permeability.

The positive correlation between low water absorption and high density indicates improved microstructural compactness through ideal binder choice and ratio adjustment. The best balance was exhibited in the GA, WS (60:40), and LX, RH (60:40) mixtures, as they were strong enough to exclude water without compromising weight or flexibility. The general conclusion is that to obtain long-term stability and dimensions of the binder in humid or outdoor environments, it is necessary to pay attention to the binder chemistry and filler morphology. Overall, the results of the SEM and FTIR analyses verified that the water absorption level is dominated by the compactness, bonding, and hydrophobic/hydrophilic properties of the matrix system. The reduced water absorption of the LX-based composites shows their effectiveness in protecting palm trunks from damage caused by moisture, especially in outdoor applications.

These are exactly the behaviors expected from previous research on sustainable lignocellulosic composites, where it was demonstrated that binder-saturated compositions or hydrophobic modifications significantly enhanced stability to densities and regulated moisture retention [3, 12, 17, 19].

3.3 Discussion of adhesion strength and linear shrinkage results

Table 5 lists the linear shrinkage and adhesion strength of the biocomposite fillers. The results clearly indicate that both the type of binder and the shape of the filler significantly influence the results. Linear shrinkage is used to show stability in the dimensions of the formation through drying and curing, and adhesion indicates the strength with which the biocomposite and substrate bond at the interface. These two factors are important for rehabilitation [3, 12, 18] and long-term performance. As shown in Table 5, the adhesion strength was significantly higher when the binder content (60:40 FB-H) was high. For instance, the adhesion strength increased from 1.25 MPa (A1) to 2.62 MPa (A4), indicating an improvement of 109.6% with increasing binder content. SEM micrographs confirmed that the properties of the composites improved with increasing binder content, showing a more continuous and well-bonded matrix with fewer interfacial defects. This indicates that the surface bonding and continuity of the matrix film were enhanced. Among all binders, GA and LX showed the highest adhesion values. GA-WS (A4) showed a maximum adhesion strength of 2.62 MPa, which is 9.2% higher than that of LX-WS (A6). The results of the FTIR analysis also indicate that there are strong hydrogen bonds (O–H groups) that support this behavior. PG, on the other hand, had worse bonding. Owing to its ability to form a continuous film because of its viscous polysaccharide structure, which affects the interfacial anchorage of the fillers with lignocellulosic fillers, it is better suited [19]. Because the elastic polymeric network of LX remains in contact even when it is bent or elongated to the extent of breaking the bond, there is also a high level of adhesion [4, 19]. However, once dried, the hydrophilic starch film of the PG solution was brittle, which led to the formation of microcracks, and it was difficult to get the two surfaces to cling to each other. The SEM images of the PG-based composite material revealed cracks and discontinuities in the matrix material. This is the reason for the reduced adhesive strength. This agrees with the results of Rahmani et al. [2] and Pedreño-Rojas et al. [20]. The type of filler also influences the adhesion level. WS composites work better than RH systems owing to their fibrous and irregular shapes and the ability to mechanically interlock and bond together. For example, GA–WS (A4) has approximately 13.9% higher adhesion strength compared to natural latex-rice husk (LX–RH) (B6), with 2.62 MPa compared to 2.15 MPa. This is in accordance with the SEM study, where the fibrous structure of the WS improved the mechanical interlocking at the interface. The adhesion strength was also lower owing to the smoother surface characteristics of RH, where the concentration of silica was higher, and the binder penetrated less [5, 16]. The smoother surface characteristics of the particles, along with the weaker interfacial contact, were also identified for the RH-based composites using SEM analysis. Unlike adhesion, the values of linear shrinkage in Table 5 have the opposite direction. The largest amount of shrinkage (up to 1.9 percent) was recorded in the case of the PG-based composites, with the lowest level of shrinkage (less than 1.0 percent) observed in the cases of GA-based and LX-based systems. For instance, the reduction in shrinkage values is from 1.65% (A1) to 0.72% (A4), which is a reduction of 56.4% owing to the increased binder content. This reduction can be attributed to the improved matrix continuity, as observed using SEM, which reduces the internal voids and, consequently, capillary stresses during the drying process. The observed behavior was a result of the drying properties of each binder. Rapid water loss results in capillary stress and contraction of hydrophilic starch matrices (PG) [12].

Table 5. Adhesion strength and linear shrinkage results of biocomposite fillers at 28 days

Mix Code	Adhesion Strength (MPa)	Linear Shrinkage (%)
A1	1.25 ± 0.05	1.65 ± 0.06
A2	1.78 ± 0.06	1.20 ± 0.05
A3	2.05 ± 0.07	0.95 ± 0.04
A4	2.62 ± 0.08	0.72 ± 0.03
A5	1.92 ± 0.06	0.80 ± 0.04
A6	2.30 ± 0.07	0.65 ± 0.03
B1	1.08 ± 0.04	1.80 ± 0.07
B2	1.55 ± 0.05	1.35 ± 0.05
B3	1.90 ± 0.06	1.10 ± 0.04
B4	2.40 ± 0.07	0.85 ± 0.03
B5	1.65 ± 0.05	1.00 ± 0.04
B6	2.15 ± 0.06	0.70 ± 0.03

However, the more evenly distributed internal stress within the LX chains and semiflexible GA network prevents any changes in dimensions. According to Teuber [16] and Subbiah Jeeva et al. [6], flexible organic binders are beneficial for shrinkage control. The RH-based composites exhibited more shrinkage than the WS-based composites. For example, the RH-based systems, such as B1 = 1.80%, showed approximately 9.1 % higher shrinkage values compared to the WS-based systems, such as A1 = 1.65%. This is due to fewer mechanical constraints during drying and friction between the layers.

Table 5 shows that adhesives with higher strengths generally exhibited lower shrinkage. It was noted that there is an inverse proportion, whereby the increase in the adhesion strength from 1.25 MPa up to 2.62 MPa was related to the decrease in shrinkage from 1.65% down to 0.72%. From the above analysis, it can be concluded that the overall SEM and FTIR analyses confirmed the above statement, that is, strong interfacial bonding and microstructure result in higher adhesion along with lower shrinkage. This phenomenon is

related to weaker interfacial bonds and porosity, as observed by SEM for systems based on RH. Owing to their adhesive strength and low shrinkage, the optimal composites were GA-WS 60:40 and LX-RH 60:40. The high adhesion strength shows that the composite materials have good bonding characteristics with wooden materials, which is important in integrating palm trunk structures.

These results are consistent with previous research on bio-based polymer composites, which showed that creating cohesive, elastic matrices, gum, and latex binders improves the durability and moisture resistance of these types of materials [3, 4, 19]. The above findings confirm that binder chemistry and content must be optimized to maintain mechanical and dimensional stability in sustainable rehabilitation materials.

3.4 Discussion of thermal conductivity result

Table 6 presents the thermal conductivity test results for the biocomposite fillers. The measured λ values were between 0.115 and 0.182 W/m·K, which is characteristic of the low thermal conductivity of lightweight lignocellulosic composites [2, 5, 12, 18]. For example, the lowest value, B6 = 0.115 W/m·K, is approximately 36.8% lower than the highest value, A1 = 0.182 W/m·K, indicating a significant variation in insulation ability based on the composition. These results indicate the appropriateness of the developed materials for the thermal insulation and rehabilitation of buildings with high-rise and fall temperatures. The thermal performance of the filler was most affected by its type. The thermal conductivity of RH composites is lower than that of WS composites (0.135–0.182 W/m·K). For example, the RH-based composite material (B6 = 0.115 W/m·K) showed a reduction of 15.4% in thermal conductivity compared to the WS-based composite material (A6 = 0.135 W/m·K), which proved the effectiveness of RH-based systems as thermal insulation. This phenomenon has been directly confirmed by SEM images, where RH-based composites show a porous structure with higher air entrapments, leading to a reduction in heat transfer. RH acted in this manner because of its porous microstructure and high silica content. They reduce the heat-transfer rate and entrap air within the matrix [5, 16]. Microscopic pores in RH provide thermal resistance, disrupt the transport of phonons in the solid matrix, and facilitate the work of plant-based composites by Rahmani et al. [2] and Parmar et al. [5]. However, the conduction of WS particles is slightly higher because they are denser and fibrous, which means that they have more contact with each other. SEM images of the WS-based composites also confirm a denser and more interconnected structure, which enhances the heat conduction pathways. This pattern was previously observed by Teuber [16] for wood-plastic composites. The chemistry also affects the reaction of the binder with heat. LX composites are less conductive than those with PG or GA. For example, LX–RH (B6 = 0.115 W/m·K) showed approximately 17.9% lower conductivity than GA–WS (A4 = 0.140 W/m·K), indicating the effectiveness of latex in enhancing thermal insulation. This is explained by the microstructure that is apparent in the SEM images, where a continuous latex matrix contains air voids and reduces the thermal conductivity. During mixing, the rubber-like elastic framework of the LX entraps air bubbles, which have lower values of qλ and are thermal insulators [19]. However, the conductivity of the PG-based systems was the highest owing to the thicker films with more starch, which offered increased channels through which heat could be conducted. The SEM images of the PG-based composite materials show relatively continuous solid phases and fewer air voids, which account for the high thermal conductivity of the materials. Formulations based on the GA did not perform well, being moderately dense and slightly flexible. These findings are consistent with those of Jefferson Andrew et al. [4] and Fong et al. [13], who reported a decrease in the overall thermal conductivity of hybrid organic composites of flexible biopolymers. The thermal conductivity decreased slightly and steadily with increasing binder content (70:30 to 60:40). For example, the thermal conductivity was reduced from 0.182 W/m·K (A1) to 0.140 W/m·K (A4), indicating a reduction of approximately 23.1% with an increase in binders. This trend is consistent with the observations made in the SEM analysis, which indicated that a higher binder content resulted in better encapsulation of particles and a controlled distribution of porosity. The detached pores were partly occupied by the denser phase of the binder, making the contact between particles slightly more enhancing the heat conduction. Enhanced trapping of air in latex systems and gum-based systems better counteracts cohesion; however, maintaining values of 9. The stability of the entrained porosity versus compaction shows the incompatibility between the densification of the matrix and thermal insulation by the entrapment of air. Krumins et al. [18] and Krišťák and Réh [17] often address bio-based building materials. In general, Table 6 proves that the thermal conductivities of all the studied composites are much lower than 0.20 W/m·K. This implies that they can be used as lightweight insulation materials. The lowest-valued λ-mixes, RH-LX (B6) and GA-RH (B4), were highly bound and had low densities. Overall, SEM and FTIR analyses confirmed that reduced thermal conductivity is governed by porosity, air entrapment, and the nature of binder-filler interactions. This implies that they can be used as thermal regulators and structural fillers for the restoration of hollow palm trunks and other natural structures. The low thermal conductivity of the developed composite materials shows their effectiveness in insulating palm trunks from heat, especially in regions with extreme temperatures. These results are in line with previous studies that have established that bio-based binders and lignocellulosic fillers can be used to make thermally stable, environmentally friendly materials for use in sustainable buildings [3, 12, 17, 19].

Table 6. Thermal conductivity results of the biocomposite fillers at 28 days

Mix Code	Thermal Conductivity (W/m·K)
A1	0.182 ± 0.005
A2	0.168 ± 0.004
A3	0.155 ± 0.004
A4	0.140 ± 0.003
A5	0.150 ± 0.004
A6	0.135 ± 0.003
B1	0.150 ± 0.004
B2	0.138 ± 0.003
B3	0.130 ± 0.003
B4	0.120 ± 0.002
B5	0.125 ± 0.003
B6	0.115 ± 0.002

3.5 Discussion of microstructural analysis (SEM)

The microstructural characteristics of the optimized biocomposite preparations were investigated by SEM, as

illustrated in Figures 1 and 2 for the GA 60:40 and LX 60:40 composites, respectively. The two fundamentally different microstructural architectures of these two systems are dictated by the morphology of the lignocellulosic filler and the type of binder, and represent the best-performing formulations of each category. Figure 1 shows that the GA-WS composite had a dense, compact, and highly cohesive microstructure. The wood fibers were deeply embedded in the GA binder matrix, forming a homogenous coating that effectively filled most of the interstitial spaces. The tight and well-integrated interfacial region between the wood fibers and GA matrix, which does not display any discernible debonding gaps or microcracks, is a good indication of strong interfacial adhesion. The close packing of particles and high level of matrix continuity were attested by the close internal architecture of the structure and low porosity rates. This thick morphology suggests that GA is a microstructural densification agent that enhances the stress transfer between the matrix and fibrous filler, in addition to acting as a binder. Such a tight and well-knit microstructure (Tables 3 and 4) is attributed to the high compressive strength and low water absorption values observed in this composite. Rahmani et al. [2] and Teuber [16] also described the dense and well-integrated microstructure in natural polymer-wood systems in similar large-scale studies, in which polymer coating and mechanical interlocking were known to be among the primary causes of enhanced structural integrity and load-bearing efficiency. In contrast, the microstructural arrangement of the LX–RH composite shown in Figure 2 is dominated by a porous and elastomeric polymer network. The LX binder formed an uninterrupted elastic film layer around the RH particles and bonded them together, over which an interconnected polymeric network was built. However, one can note that the matrix had a large population of pores and voids. These pores are also associated with the morphology of the rice husk particles and the inherent nature of latex in forming films, which are relatively well distributed. Although no dense packing was observed in the GA–WS system, the interfaces between the latex and rice husks appeared smooth and well-bonded, indicating that they were physically bonded well. The porous and open structure allows the composite to sustain localized deformation and microstrains without being easily broken due to its more porous and open structure. These microstructural features explain the low linear contraction and high adhesion of the system (Table 5). Moreover, the low thermal conductivity of this composite is partly due to the dispersed pores and network of the elastic polymer structure, as the air trapped in the pores forms a good thermal resistance barrier and hinders the pathways of heat transfer within the material [19].

A direct comparison of these two figures shows that the binder type has a significant effect on the final microstructure of the composite material. The latex system produced an open and porous structure that was more flexible. However, the use of a GA binder system produces a dense and compact structure that is stiffer, has a strong interfacial bond, and has minimal porosity. The macroscopic properties of these two binder systems are consistent with their respective microstructures: the GA-WS composite is more suited for applications requiring high strength, stiffness, and low permeability, whereas the LX-RH composite is more suited for applications requiring flexibility and deformation tolerance, as well as for thermal insulation.

From the SEM analysis of these two composite systems, it is evident that the significant microstructural characteristics that affect the performance of the formed biocomposites include the pore structure, continuity of the matrix phase, and compatibility between the binder and filler interfaces. The latex system was more flexible and resilient, whereas the GA system was more compact and rigid. These two composite systems are more suited for environment-friendly rehabilitation applications that require simultaneous mechanical and thermal performance owing to their combined characteristics [3, 12, 19].

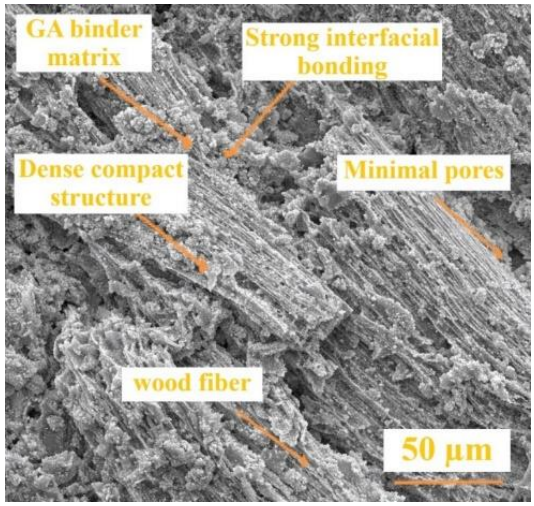

Figure 1. The SEM image of GA–WS (60:40) shows a dense, compact structure and strong interfacial bonding

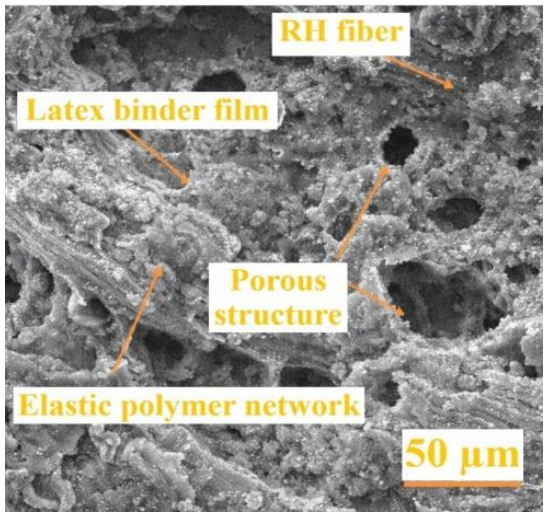

Figure 2. The SEM image of natural latex-rice husk (LX–RH) (60:40) shows a porous elastic polymer network with rice-husk particles

3.6 Discussion of FTIR analysis

FTIR spectra of GA, GA–WS, LX, and LX–RH composites are presented in Figures 3 and 4. The functional groups present in the binders and the nature of the interaction between the binders and lignocellulosic fillers were identified. The broadband present at a wavenumber between 3400 and 3300 cm^{-1} is related to the presence of hydroxyl groups, as indicated by the presence of O–H stretching vibrations. The higher intensity of the band is related to the presence of hydroxyl groups, which are present in polysaccharides, cellulose, and moisture. The presence of absorption bands at wavenumbers

between 2920-2850 cm^{-1} is related to the presence of aliphatic hydrocarbons, as indicated by the presence of C–H stretching vibrations. The increased intensity of the band is related to the presence of more carbon atoms, which are present in lignocellulosic materials. The band present at approximately 1640 cm^{-1} is related to the presence of water molecules, as indicated by the presence of H–O–H bending vibrations, as well as the presence of conjugated carbonyl groups.

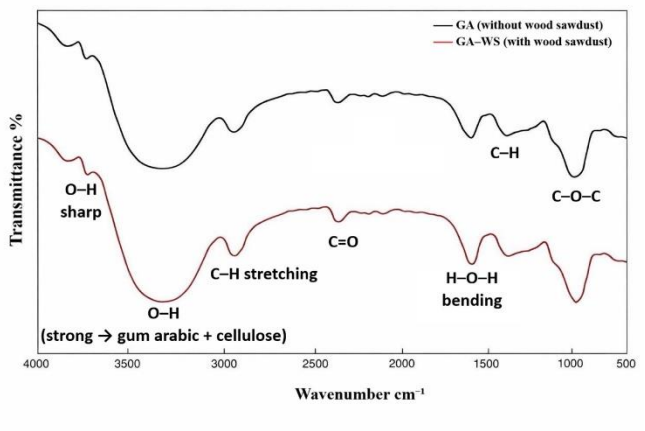

Figure 3. FTIR spectra of gum arabic (GA) and gum arabic-wood sawdust (GA–WS) composites showing similar spectral features and physical interaction dominated by hydrogen bonding

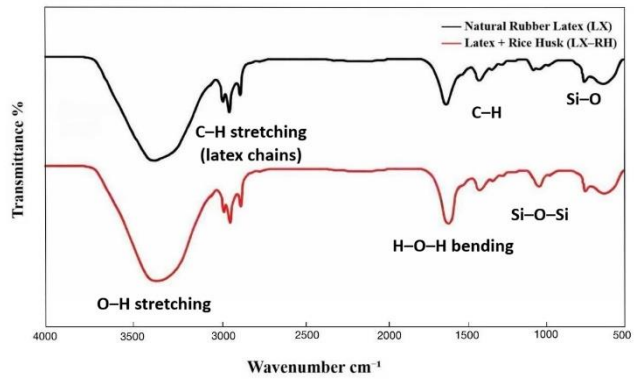

Figure 4. FTIR spectra of natural latex (LX) and natural latex-rice husk (LX–RH) composites, confirming the physical incorporation of rice husk (RH) into the latex matrix

The weak band present at a wavenumber of approximately 1730 cm^{-1} is related to the presence of ester or carboxyl groups, which are present in GA. A prominent band in the range of 1050 to 1030 cm^{-1} can be attributed to the Si-O-Si stretching vibration due to silica in RH and the C-O-C stretching vibration due to cellulose.

Most importantly, when comparing the composite spectrum with those of the individual binders, no new absorption bands were noticed. Similarly, no changes in the peaks were observed. This further confirms that no new chemical bonds are formed during the interaction of the binders with the fillers. Therefore, it can be confirmed that physical interactions are predominant in the interaction between the binders and fillers. These physical interactions are in line with those observed in the interface region in the SEM images (Figures 1 and 2).

A weak absorption band was observed in the range of 2330–2350 cm^{-1}. This can be attributed to CO_2 in the atmosphere. CO_2 was present in the optical path during FTIR spectroscopy. Similarly, CO_2 can also be entrapped in the structure of composite materials owing to their porosity. In the FTIR spectrum of the GA-WS composite, this band is more pronounced due to its high porosity and carbon content. However, in the FTIR spectrum of the LX-RH composite, this band is not pronounced owing to its low porosity compared to WS.

The FTIR spectra further confirmed that both biocomposites retained their original chemical structure. The compatibility of binders with fillers is primarily due to their physical interactions.

3.7 Discussion of thermogravimetric and differential scanning calorimetry analyses

Thermal analysis was performed to assess the thermal stability of the prepared biocomposites within and beyond their service temperature limits (≤ 60 °C). The TGA and DSC plots of the selected biocomposites, GA-WS (A4) and LX-RH (B6), are shown in Figures 5 and 6.

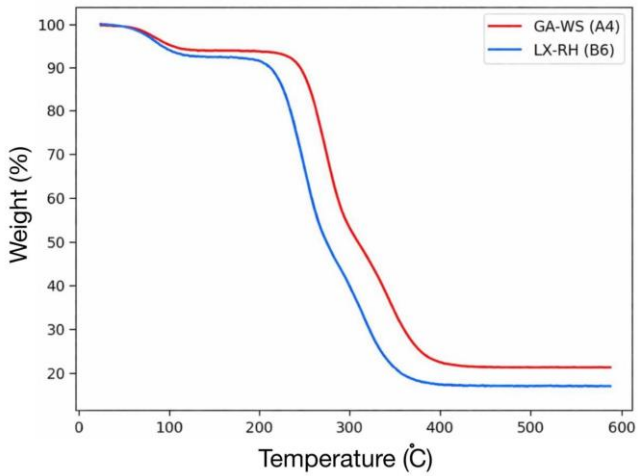

Figure 5. The thermogravimetric analysis (TGA) curves of the GA-Ws and LX-RH composites indicate the weight loss behavior and thermal stability of the composites

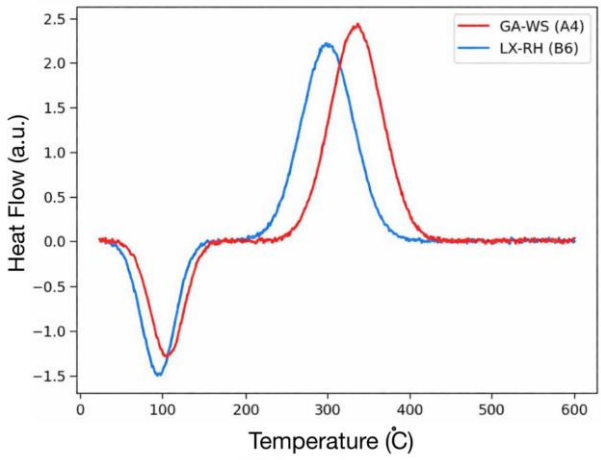

Figure 6. Differential scanning calorimetry (DSC) thermograms of GA-Ws and LX-RH composites, indicating the thermal transitions of the composites

Three distinct weight loss regions were observed in the TGA plots of the biocomposites. The first weight loss region is due to the evaporation of physically held moisture within the temperature range of 25-120 ℃, resulting in a weight loss of 4-6%, due to the hydrophilic properties of lignocellulosic materials [2, 12]. The second weight loss region is due to the thermal degradation of hemicellulose and binder within the temperature range of 230-370 ℃ [4, 19]. The third weight loss region is due to the thermal degradation of lignin and formation of char at temperatures above 400 ℃, resulting in a high residual mass at elevated temperatures [12, 17]. For instance, the mass loss during the initial stage was found to be 4.8% for GA-WS (A4), whereas it was 5.2% for LX-RH (B6), indicating that LX-RH had an increase of approximately 8.3% in moisture weight loss compared to GA. This is in line with the FTIR test results, which indicate that the presence of hydrophilic O-H groups in GA-based systems is responsible for the retention of moisture and the control of evaporation behavior.

It is also noted that within the service temperature limits (≤ 60 ℃), negligible weight loss (< 0.5%) is observed for the biocomposites, indicating their thermal stability at practical working temperatures. The slightly higher residual mass of the GA-WS system indicates higher char formation and thermal stability than those of the LX-RH system. In this regard, it can be clearly stated that LX-RH (22.3%) shows approximately 14.4% higher values in residual mass compared to GA-WS (19.5%) at 600 ℃. This is related to the microstructural differences identified in the SEM images, in which a denser carbonaceous microstructure is identified for the GA-based systems, and a more flexible matrix is identified for the LX-based systems.

The DSC thermograms also verified these results. The endothermic peaks at 100 ℃ are related to the removal of moisture from the material [2, 12]. The broad exothermic peaks at 300-350 ℃ are related to the degradation of polysaccharide structures [4, 17]. For example, the exothermic peak shifted from 305 ℃ in GA-Ws to 335 ℃ in LX-RH, indicating an increase of approximately 9.8%, which implies a better heat resistance for the LX-based material. The shift of the exothermic peaks to higher temperatures in the LX–RH thermogram indicates differences in the thermal transitions of these two systems. This change is also supported by SEM observations of the improved structural uniformity and flexibility of the LX-based composites, which delays thermal degradation.

Most importantly, no significant thermal transitions were detected in these biocomposites at temperatures lower than 150 ℃, which verifies the absence of premature degradation or instability of these biocomposites under ambient or service conditions. These results show that the proposed biocomposites have sufficient thermal stability for use under mild environmental conditions. Additionally, the temperature range for the occurrence of major degradation increased from 245 ℃ for GA-WS to 260 ℃ for LX-RH, which is equivalent to an increase of 6.1%, thus proving the enhanced thermal stability of the LX-RH composite materials. In conclusion, the SEM and FTIR results indicate that the thermal stability of the materials depends on the binder-filler interaction, compactness of the microstructure, and nature of the organic constituents of the matrix material.

As a summary of the results obtained from the analysis of the thermal stability of these biocomposites using TGA and DSC, a table of the important parameters obtained from these tests is shown in Table 7.

The general behavior of the developed biocomposites can be explained by considering the overall impact of the chemistry of the binder, morphology of the filler particles, and characteristics of the microstructure. Specifically, the hydrophobic nature of latex minimizes moisture absorption by creating a continuous impermeable film, whereas fibrous WS improves the mechanical interlocking effect, and the presence of silica in RH affects bonding. This proves that the developed composite materials can reduce the rate of heat transfer in palm trunk structures, thus insulating and protecting them from extreme temperature fluctuations in arid regions.

Table 7. Summary of thermogravimetric analysis (TGA) and differential scanning calorimetry (DSC) results for representative biocomposite formulations (A4 and B6)

Parameter	A4 (GA–WS, 60:40)	B6 (LX–RH, 60:40)
Initial mass loss (moisture evaporation) range (℃)	30–110	35–120
Mass loss in this range (%)	4.8	5.2
Onset of major degradation (℃)	245	260
Peak degradation temperature (℃)	312	328
Residual mass at 600 ℃ (%)	19.5	22.3
DSC endothermic peak (moisture release, ℃)	98	104
DSC exothermic transition (polymer decomposition, ℃)	305	335
Observed mass loss up to 60 ℃ (%)	<0.5	<0.5
Thermal stability within service range (≤ 60 ℃)	Stable	Stable

3.8 Statistical analysis

The results obtained for all experiments are presented as mean values ± standard deviation for n = 3 replicates for each formulation. One-way analysis of variance (ANOVA) was performed for each measured property for all 12 formulations ($k = 12$, $df_{between} = 11$, $df_{within} = 24$). To find statistically significant differences between groups, a post-hoc Tukey's Honestly Significant Difference (HSD) test was performed for each property at a confidence level $\alpha = 0.05$. Values with the same superscript letter are not significantly different ($p > 0.05$).

The results obtained through analysis of variance (ANOVA) for all properties, as shown in Table 8, indicate that statistically significant differences exist among all formulations for all properties ($p < 0.001$). The values for the F-tests were as follows: compressive strength, $F(11, 24) = 100.46$; water absorption, $F(11, 24) = 91.02$; bulk density, $F(11, 24) = 11.92$; adhesion strength, $F(11, 24) = 169.23$; linear shrinkage, $F(11, 24) = 214.68$; and thermal conductivity, $F(11, 24) = 98.80$. The high values of the F-tests indicate that the differences are statistically significant and are controlled primarily by the formulation parameters.

The results obtained through Tukey's HSD analysis were consistent for all properties. The GA-based composites exhibited significantly higher compressive and adhesion strengths than the PG-based composites ($p < 0.001$). The LX-based composites showed relatively higher water absorption and lower thermal conductivity than the GA-based composites, indicating a more porous and flexible structure. The WS-based composites showed significantly higher

strengths than the RH-based composites. The 60:40 binder content resulted in a statistically significant improvement in the strength and a decrease in the water absorption ($p < 0.001$).

The results obtained through this analysis confirm that the binder type is the major factor that influences most properties, followed by the binder content and filler type. The results obtained through this analysis strongly confirm that the trends discussed in Sections 3.1 to 3.4 are statistically significant. Owing to space limitations, significance groupings from Tukey's HSD test are not explicitly indicated in the tables, but were considered in the statistical interpretation.

Table 8. Summary of one-way ANOVA results for all measured properties (k = 12 groups, n = 3 replicates per group)

Property	SSB	SSW	MSB	F (11, 24)	p-value
Compressive Strength (MPa)	25.02	0.543	2.275	100.46	< 0.001
Water Absorption (%)	108.47	2.600	9.861	91.02	< 0.001
Bulk Density (kg/m³)	40808.75	7468.00	3709.89	11.92	< 0.001
Adhesion Strength (MPa)	6.919	0.089	0.629	169.23	< 0.001
Linear Shrinkage (%)	4.625	0.047	0.420	214.68	< 0.001
Thermal Conductivity (W/m·K)	0.0129	0.000284	0.00117	98.80	< 0.001

Notes: SSB = sum of squares between groups; SSW = sum of squares within groups; MSB = mean square between groups. $df_{between} = 11$ and $df_{within} = 24$ for all tests. The units of the SSB and MSB match the units of each property squared.

4. CONCLUSION

The results indicate that the performance of the developed biocomposites is largely influenced by the type of binder material as well as the morphology of the filler material. Increasing the proportion of the binder material to 60:40 enhanced the continuity of the matrix material, reduced the porosity, and improved the performance. The GA-WS composite had the highest compressive strength at 5.8 MPa and the lowest water absorption at 8.1%. This is because of the dense structure, which allows for improved interfacial bonding. On the other hand, the LX-RH composite had relatively low thermal conductivity at 0.115 W/m·K, higher adhesion at 2.15 MPa, and lower shrinkage at 0.70%. This is because of the porous structure, which allows for improved flexibility. According to the results, it was observed that the interaction between the components was physical rather than chemical, as confirmed by FTIR analysis. According to the results, GA-based composites are more suitable for use in applications requiring improved strength and reduced permeability. On the other hand, LX-based composites are more suitable for use in applications requiring improved thermal insulation and deformation tolerance.

ACKNOWLEDGMENT

The authors sincerely thank Mustansiriyah University for providing the facilities and assistance used in this study.

REFERENCES

[1] Kaptan, A., Kartal, F. (2024). A critical review of composite filaments for fused deposition modeling: Material properties, applications, and future directions. European Mechanical Science, 8(3): 199-209. https://doi.org/10.26701/ems.1451829

[2] Rahmani, H., Algirdas, A., Shestavetska, A., Vaiciukyniene, D. (2025). Preparation and mechanical characterization of pressed carbonized wood sawdust bio-composite. Scientific Reports, 15(1): 14981. https://doi.org/10.1038/s41598-025-98658-w

[3] Aiduang, W., Jinanukul, P., Thamjaree, W., Kiatsiriroat, T., Waroonkun, T., Lumyong, S. (2024). A comprehensive review on studying and developing guidelines to standardize the inspection of properties and production methods for mycelium-bound composites in bio-based building material applications. Biomimetics, 9(9): 549. https://doi.org/10.3390/biomimetics9090549

[4] Jefferson Andrew, J., Sain, M., Ramakrishna, S., Jawaid, M., Dhakal, H.N. (2024). Environmentally friendly fire retardant natural fibre composites: A review. International Materials Reviews, 69(5-6): 267-308. https://doi.org/10.1177/09506608241266302

[5] Parmar, N., Vats, A., Devi, V., Kwatra, S., Srivastava, R.K., Singh, S.B. (2024). Assessing the sustainability and performance of hempcrete. International Journal of Environment and Climate Change, 14(7): 609-622. https://doi.org/10.9734/ijecc/2024/v14i74299

[6] Subbiah Jeeva, G., Darwin, J.D., Thangadurai, B., Aravinth, M., Amala Jenix, M. (2023). Experimental investigation on effect of ground nut husk filler in banana fiber reinforced polymer composite and its application. International Journal of Engineering Technology and Management Sciences, 7(2): 836-840. https://doi.org/10.46647/ijetms.2023.v07i02.092

[7] Tibaduiza Burgos, D.A., Gomez Vargas, R.C., Pedraza, C., Agis, D., Pozo, F. (2020). Damage identification in structural health monitoring: A brief review from its implementation to the use of data-driven applications. Sensors, 20(3): 733. https://doi.org/10.3390/s20030733

[8] Ewart, P. (2020). A comparison of processing techniques for producing prototype injection moulding inserts. In Proceedings of Innovations in Manufacturing and Design Conference, Waikato Institute of Technology. http://researcharchive.wintec.ac.nz/id/eprint/7270.

[9] D'Amato, D., Veijonaho, S., Toppinen, A. (2020). Towards sustainability? Forest-based circular bioeconomy business models in Finnish SMEs. Forest Policy and Economics, 110: 101848. https://doi.org/10.1016/j.forpol.2018.12.004

[10] Crespo-Herrera, L.A., Ortiz, R. (2015). Plant breeding for organic agriculture: Something new? Agriculture & Food Security, 4(1): 25. https://doi.org/10.1186/s40066-015-0045-1

[11] Pickering, K.L., Efendy, M.G.A., Le, T.M. (2016). A review of recent developments in natural fibre composites and their mechanical performance. Composites Part A, 83: 98-112. https://doi.org/10.1016/j.compositesa.2015.08.038

[12] Musioł, M., Jurczyk, S., Sobota, M., Klim, M., Sikorska, W., Zięba, M., Janeczek, H., Rydz, J., Kurcok, P., Johnston, B., Radecka, I. (2020). (Bio)degradable polymeric materials for sustainable future—Part 3:

Degradation studies of the PHA/wood flour-based composites and preliminary tests of antimicrobial activity. Materials, 13(9): 2200. https://doi.org/10.3390/ma13092200
[13] Fong, A., Wong, D.H., Lau, S., Debnath, S., Anwar, M., Davies, I.J., Johar, M.B. (2025). A review on the hybrid polymer composites comprising natural fibre and nanomaterial reinforcement. Journal of Composite Materials, 59(22): 2615-2646. https://doi.org/10.1177/00219983251334861
[14] Rosentrater, K.A. (2007). Ethanol processing co-products: Economics, impacts, sustainability. NABC, USDA/ARS North Central Agricultural Research Laboratory.
[15] Giurca, A., Jonsson, K.H.R., Lovric, M., Pepke, E. (2014). European Union timber regulation impact on international timber markets. Technical University in Zvolen, pp. 105-119. https://doi.org/10.13140/2.1.4837.2003
[16] Teuber, L. (2016). Evaluation of particle and fibre degradation during processing of wood plastic composites (WPC) using dynamic image analysis. Doctoral dissertation, University of Göttingen. https://doi.org/10.53846/goediss-5800
[17] Krišťák, Ľ., Réh, R. (2021). Application of wood composites. Applied Sciences, 11(8): 3479. https://doi.org/10.3390/app11083479
[18] Krumins, J.A., Vamza, I., Dzalbs, A., Blumberga, D. (2024). Particle boards from forest residues and bio-based adhesive. Buildings, 14(2): 462. https://doi.org/10.3390/buildings14020462
[19] Aman, A., Yeneneh, K., Shemsedin, A., Zegale, B., Wakshume, E. (2025). Development and optimization of a bio-based adhesive from Euphorbia trigon latex reinforced with alumina for sustainable wood bonding applications. Results in Engineering, 27: 106468. https://doi.org/10.1016/j.rineng.2025.106468
[20] Pedreño-Rojas, M.A., Morales-Conde, M.J., Rubio-de-Hita, P., Pérez-Gálvez, F. (2019). Impact of wetting–drying cycles on the mechanical properties and microstructure of wood waste–gypsum composites. Materials, 12(11): 1829. https://doi.org/10.3390/ma12111829

NOMENCLATURE

Abbreviations

WS	Wood Sawdust
RH	Rice Husk
GA	Gum Arabic
PG	Plant-based Glue
LX	Natural Rubber Latex (NRL)
FB-L	A Low Binder Fraction (Filler: Binder = 70:30 wt.%)
FB-H	A High Binder Fraction (Filler: Binder = 60:40 wt.%)
SEM	Scanning Electron Microscopy
FTIR	Fourier Transform Infrared Spectroscopy
TGA	Thermogravimetric Analysis
DSC	Differential Scanning Calorimetry
NRL	Natural Rubber Latex

Greek Symbols

λ	Thermal conductivity (W/m·K)

Subscripts

A	Group A composites (Wood Sawdust-based)
B	Group B composites (Rice Husk-based)
A1–A6	Wood Sawdust mix codes (PG, GA, LX at 70:30 and 60:40 ratios)
B1–B6	Rice Husk mix codes (PG, GA, LX at 70:30 and 60:40 ratios)

Key Parameters

MPa	Megapascal (unit of compressive and adhesion strength)
W/m·K	Watts per meter-Kelvin (unit of thermal conductivity)
kg/m³	Kilograms per cubic meter (unit of bulk density)
wt.%	Weight percent
℃	Degrees Celsius